



OPEN An optimal multi-objective control architecture of PMSM drives

Biplab Kumar Mohapatra, Vidit Sharma, Pritam Bhowmik & Rupa Mishra✉

This study proposes an optimal multi-objective control architecture for salient permanent magnet synchronous motors (PMSM) drives. It is aimed at improving overall system performance and energy efficiency in electric vehicle applications. The Vector Model Predictive Control (V-MPC) method enhances robustness under parameter mismatches and load variations, indirectly supporting efficient energy use. In this study, a current-based rotor angle estimation is proposed to enhance the robustness during large load torque variation of the drive. The model employs a step ahead algorithm with unit delay compensation, ensuring mathematical stability and efficacy within the boundaries to manage nonlinear restraints effectively. The 4-sector modified voltage vector selection by using current error optimization is included in this work to reduce the enumeration process and improve the drive performance. This recursion-based stator-current step ahead model by using V-MPC is established to reduce ripples and harmonics in stator current. Moreover, the multi-objective cost function is able to maintain the machine variables during parameter mismatching by increasing system performance. Furthermore, the stability analysis by using Lyapunov energy function are provided in theory. The theoretical claims are validating the feasibility of the proposed scheme in the Simulink MATLAB environment.

Keywords Permanent magnet synchronous motor (PMSM), Voltage control, Predictive control, Electric vehicle (EV)

Permanent magnet synchronous machines (PMSMs) have been broadly used in industrial and transportation fields due to the merits of compact structure, high control accuracy, torque balance, and high efficiency, as well as high reliability^{1,2}. Their compact size and ability to deliver high torque make them a preferred choice in electric vehicles (EV)³. In accordance to use and control of PMSM various methods were implemented, one such method implemented was vector control (VC) method. Distributed in different time frames, VC methods approach towards the independent control of the motor improving the use of active and reactive power. Major key components of VC primarily focused into the regulation of speed and flux⁴. But due to use of the permanent magnet in the machine, flux variations and leakage were major issues prompting the inefficient method of control.

To cope with the integration of distributed generation system for varieties of applications, traditional control strategies are no longer enough to meet these requirements and provide the optimal performance. Control methods such as Proportional-Integral (PI), Sliding Mode Control (SMC), Fuzzy Logic Control (FLC) were reported for the controlled action of the machine^{5,6}. On the other hand, PI controllers, while simple to implement, often struggle to handle the nonlinear dynamics of PMSMs and require extensive tuning for optimal performance. Sliding Mode Control is robust against parameter variations but introduces undesirable chattering effects. Controllers like fuzzy logic heavily depend on experimental data and are not ideal for varying driving cycles in load torque varying applications.

To overcome the issue of torque ripples and current variations, direct torque control (DTC) and direct power control is implemented. DTC provided the faster and higher control of torque and flux in response to load requirement of the motor with minimal delay. However, in DTC a key limitation has occurred, which is high pulsation in torque. This is majorly caused due to the discrete selection of voltage vector during running condition of the motor. Hence DTC comes with inherent limitations despite their fast dynamic response, suffer from high torque and flux ripples, making them inappropriate for applications requiring smooth operation. These limitations often result in suboptimal performance, particularly in applications with stringent control requirements⁷.

Model predictive control (MPC) has expanded intensive consideration in the arena of motor drives^{8,9}. As MPC anticipates step ahead behavior by solving an optimization problem over a finite horizon, allowing it to handle both source and load-side variations effectively. Unlike conventional PI or deadbeat control, MPC

School of Electrical Engineering, VIT Chennai Campus, Chennai, Tamil Nadu 600048, India. ✉email: rupa.mishra@vit.ac.in

considers the dynamics of speed and torque variations, making it suitable for e-mobility applications where these variations are frequent^{10–12}. MPC is better equipped to manage nonlinearities in the system, such as those arising from the machine's saliency or mismatch of parameters. Optimal control of step ahead scheme enables precise control of the machine variables in the machine-side converter, ensuring stability in both steady-state and transient conditions. This is critical for distributed generation and EV applications, where consistent power delivery is required^{11–13}. Moreover, it ensures better dynamic conditions, enhancing overall drive efficiency.

The challenge in the predictive control is to reduce the computational burden by selecting suitable voltage vector. An active zero-state strategy is explained in¹⁴, in which two sectors are used to substitute the null vector. Due to the involvement of only active vectors amplitude is effectively suppressed. In 15–17 all non-zero vectors are used to create a

series of virtual vectors with amplitude of zero for the reduction of third harmonics. Due to the capability of including multi objective criteria in MPC, it is easy to achieve suppression of current ripple.

Therefore, this article aims to propose an improved MPC to simultaneously reduce switching loss, current abnormalities during fault for PMSM drives. Due to dependency of machine parameter during predictive control design, it adapts to changes in inductance and resistance, maintaining control accuracy. Noise and uncertainty management unlike in extended Kalman filter, which can be affected by noise due to its stochastic nature^{12–14}, MPC optimizes control actions even when terminal signals are noisy or uncertain. This makes MPC more reliable for real-time applications in frequent load torque shifting applications.

However, the reports described above all use speed sensor/observers, which will rise the economy. Therefore, in order to minimise the cost and enhance the stability, this work explores the scheme with a minimal volume capacitor and without a speed sensor, and also deliberates the instance of the dc-link voltage perturbations. So, a predictive controller for the PMSM installed in EV suitable for inclined/normal road is designed in this paper. Finally mathematical results are provided to verify the effectiveness of the proposed method.

The contributions of this paper are given as follows.

1. A recursive predictive model for machine current is constructed in rotor flux reference frame, which can diminish the computational complexity and improved steady-state control performance.
2. A Mult objective cost function is derived to select the suitable voltage vector selection in an optimal manner with additional degrees of freedom. This enables the flexible regulation and precise control to minimize the motor abnormalities.
3. In this work only four non zero voltage vector are used for optimal switching selection which reduce computation complexity.

The overall system performance is design in MATLAB-Simulink, ensuring the scheme is both operative and appropriate to real-world scenarios.

System description

The overall schematic description of the topology is shown in Fig. 1. The operation of the PMSM with power converter is controlled by the dedicated control unit, which consists of the MPC-based supervisory controller and PI regulator based local controllers. A dc voltage source is modeled here as a variable dc link voltage source supply to the whole working model. The inverter is directly responsible for the running of the permanent magnet synchronous motor.

The predictive approach uses a discrete mathematical orientation of the controlled variables to predict future state variables, enabling the selection of the optimal voltage vector (VV) to apply to the motor. In this work to generate gate signal for two-level inverter, the cost function of MPC prefers the outermost square of the voltage space vector, which allows the possibility of reducing the number of VVs. A block diagram of PMSM as shown in Fig. 2 consists of step ahead prediction of the stator current to achieve decouple control of active and reactive component of the machine and outer loop for dc-link voltage control.

The stator current sampled and transformed to dq-axis in the rotor flux reference frame. The d and q-axis components of the stator current are used to control the rotor flux linkage and the motor torque, respectively. Eventually, the inverter voltages are generated and applied to the machine as per the demand of the vehicle. Normally stator voltage synthesized here by using the equation given below:

$$u_{dqsn}(k) = s(k) V_{dc} \quad (1)$$

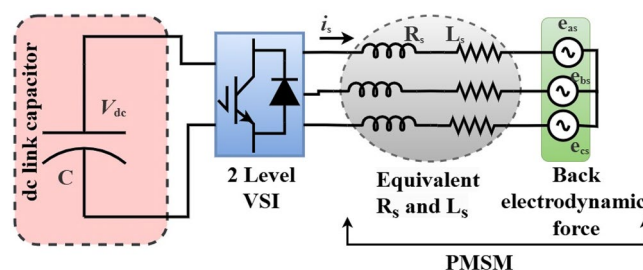


Fig. 1. Power schematic structure diagram of the platform.

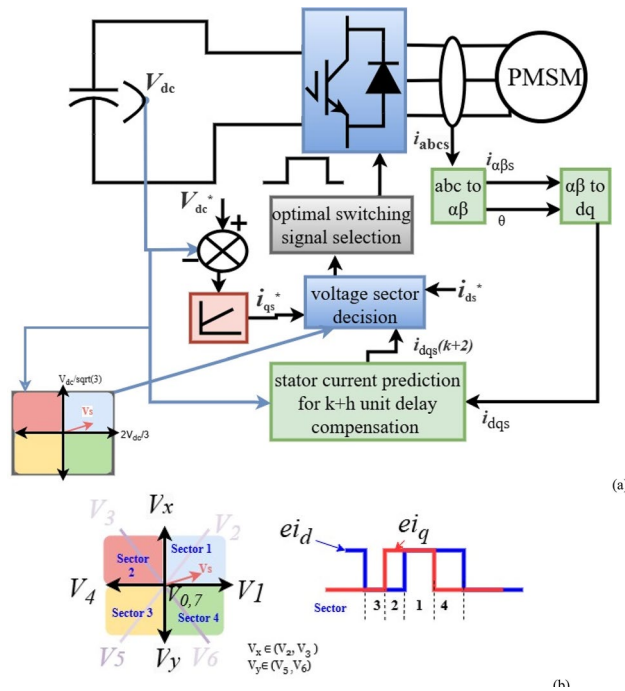


Fig. 2. (a) Control architecture of the PMSM fed drive system (b) Control algorithm for sector decision from error of dq-axis current.

$$s = \begin{cases} \frac{2}{3}e^{j((n-1)\frac{\pi}{3})+\theta}, n \in (1,2 \dots 6) \\ 0, n = (0,7) \end{cases}$$

k is the present sampling instant, θ rotor angle.

But in this case instead of generating all the 6 possible non zero voltage vector, only 4 voltage vector is synthesized as shown in the Fig. 2b. The robustness is achieved by the online optimal regulations which can adjust with parameter mismatch as presented in Fig. 3a. The stability is assured by the Lyapunov energy function. The designed controller provides the stability guarantees while dynamically correcting the source and load perturbations. To eliminate misdiagnosis of the current, in this work the objective function is designed by considering a nonlinear term. Finally, the suitable switching sector is achieved by the minimisation of cost function with unit delay compensation.

Modeling and analysis of the proposed system

The dynamic equations of PMSM can be described with state variable, i.e., stator current components and rotor flux components as¹²:

$$u_{ds} = i_{ds}R_s + L_{ds}\frac{di_{ds}}{dt} - \omega_e L_{qs}i_{qs} \tag{2.a}$$

$$u_{qs} = i_{qs}R_s + L_{qs}\frac{di_{qs}}{dt} + \omega_e L_{ds}i_{ds} + \omega_e\varphi_f \tag{2.b}$$

Now to predict the future machine behavior, the equation will be rewritten as:

$$\begin{bmatrix} \frac{di_{ds}}{dt} \\ \frac{di_{qs}}{dt} \end{bmatrix} = \begin{bmatrix} -\frac{R_s}{L_{ds}} & \omega_e \frac{L_{qs}}{L_{ds}} \\ -\omega_e \frac{L_{ds}}{L_{qs}} & -\frac{R_s}{L_{qs}} \end{bmatrix} \begin{bmatrix} i_{ds} \\ i_{qs} \end{bmatrix} + \begin{bmatrix} \frac{1}{L_{ds}} & 0 \\ 0 & \frac{1}{L_{qs}} \end{bmatrix} \begin{bmatrix} u_{ds} & 0 \\ u_{qs} & -\omega_e\varphi_f \end{bmatrix} \tag{3}$$

where u_{dq} , i_{dq} represent the machine stator voltage and current on the rotor flux reference frame (dq-axis), respectively, ω_e represents the mechanical angular speed of the motor, L_{dq} , R_s , φ_f are d-axis inductance, q-axis inductance, stator resistance and magnet flux linkage respectively.

Due to the presence of permanent magnet d-axis stator current reference is set as zero. This setting value adjustment efficiently decouples the active and reactive power components of the current. As a result, the electromagnetic torque of the motor is given by:

$$T_e = \frac{3}{2}(P\varphi_f i_{qs}) = kt i_{qs} \tag{4}$$

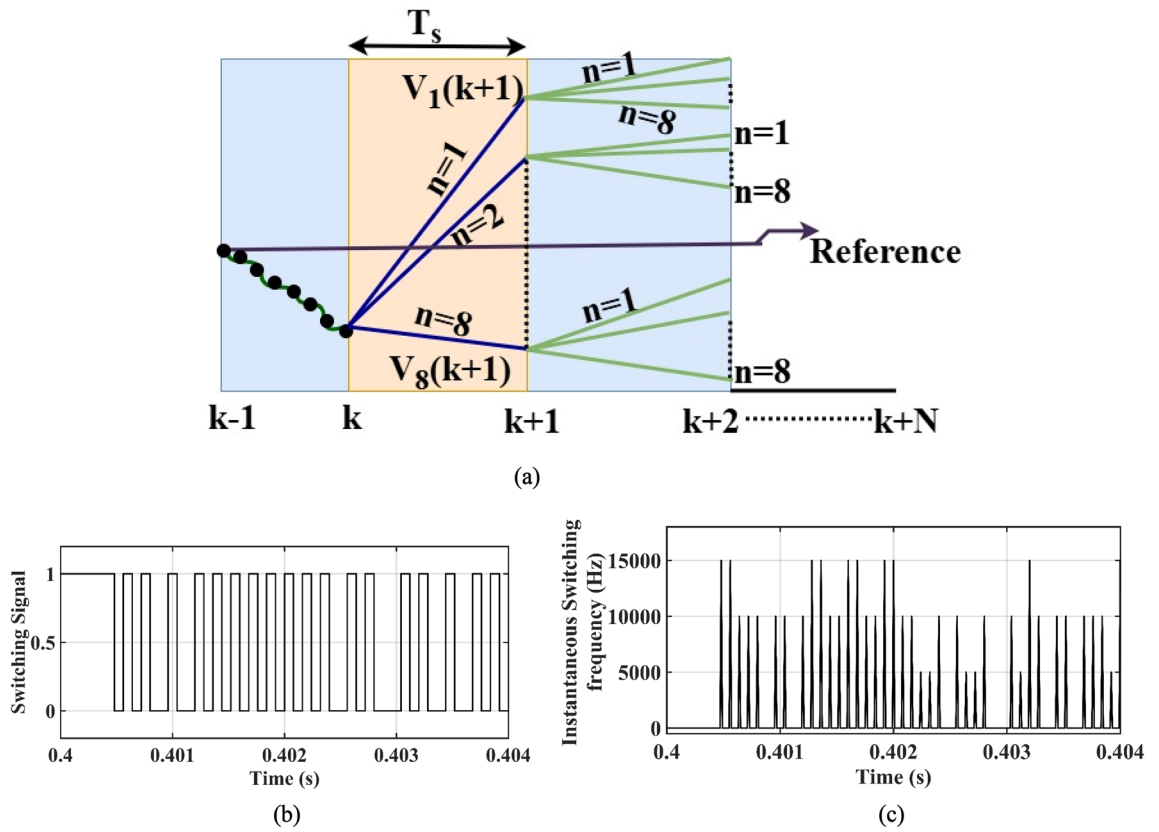


Fig. 3. (a) Data model updating and voltage prediction (b) Switching signal (c) Instantaneous switching frequency.

Thereby controlling the q-axis stator current, the torque can be regulated. The motor dynamics is given as:

$$T_e - T_L = J \frac{d\omega}{dt} + B\omega \Rightarrow \frac{d\omega}{dt} = \frac{k_t}{J} i_{qs} - \frac{T_L}{J} - \frac{B}{J} \omega \tag{5}$$

The control strategy is carried out considering the disturbances to enhance the control efficacy. Let us consider that the system disturbances are represented by the variable $\delta(t)$.

$\delta(t)$ eq axis component of the stator current error and load and frictional perturbations

Now, the motor dynamics in (5) considering the disturbances can be modified as:

$$\frac{d\omega}{dt} = \frac{k_t}{J} i_{qs} - \underbrace{\left(\frac{T_L}{J} - \frac{B}{J} \omega - \left\{ \frac{k_t}{J} (i_{qs}^{ref} - i_{qs}) \right\} \right)}_{\delta(t)} \tag{6}$$

Now to generate q-axis current instead of speed loop, the power balancing is done between machine source and load end. So, the active power of the machine at dq reference can be determined using the equations below:

$$P = \frac{3}{2} (V_{ds} i_{ds} + V_{qs} i_{qs}) \tag{7}$$

Being a permanent-magnet machine, the i_{ds} is considered as zero. Now, the equation governing the dc-link voltage dynamics is given by:

$$P = \frac{3}{2} (V_{qs} i_{qs}) = V_{dc} C \frac{dV_{dc}}{dt} \tag{8}$$

The voltage across dc link capacitor (V_{dc}) is regulated by the currents that flow in and draw out. The desired value of the dc voltage is reached considering the link between the active power flow produced by the PMSM and the change in the capacitor voltage. This relation allows to determine the reference of the q-axis current, which enables the achievement of the desired dc voltage as shown in (8). The q-axis reference current is constructed

using a PI-Controller that controls speed by means of dc link voltage loop, and is fed into the optimization algorithm of the model predictive control method. In this work the dc link voltage controller is able to mimic the behavior of machine dynamics as given in (6).

The discrete state-space model of the motor is described using the Euler method with the sampling period T_s . The continuous-time system (3) is converted in the discrete time system to predict the next step states:

$$\begin{bmatrix} i_{ds}(k+h) \\ i_{qs}(k+h) \end{bmatrix} = \begin{bmatrix} 1 - \frac{R_s T_s}{L_{ds}} & \omega_e \frac{L_{qs} T_s}{L_{ds}} \\ -\omega_e \frac{L_{ds} T_s}{L_{qs}} & 1 - \frac{R_s T_s}{L_{qs}} \end{bmatrix} \begin{bmatrix} i_{ds}(k) \\ i_{qs}(k) \end{bmatrix} + \begin{bmatrix} \frac{T_s}{L_{ds}} & 0 \\ 0 & \frac{T_s}{L_{qs}} \end{bmatrix} \begin{bmatrix} u_{ds}(k) & 0 \\ u_{qs}(k) & -\omega_e \varphi_f \end{bmatrix} \quad (9)$$

The proposed strategy minimizes the Lyapunov energy function, which is the control objective directly introduced in the objective function. The computational burden is the major problem for the implementation of MPC. So, in this case a 4 sector VV is selection is decided as per the current error (i_{dq}).

The Mult objective cost function including switch state is introduced in the objective function to reduce switching power loss. The optimal control problem is formulated by using the Lyapunov stability criterion for each allowable control input. The cost function incorporates current error reduction, switching frequency reduction, and current limitation, with empirical weighting factors for limit violation. This reduces current harmonics and results in less ripple.

The deigned control configuration minimizes the basic objective function as:

$$\lambda = \mu \lambda_1 + (1 - \mu) \lambda_2; \mu(\text{weighing factor}) \in (0,1) \quad (10)$$

$$\lambda_1 = \frac{1}{2} C \underbrace{(V_{dc}^{ref} - V_{dc})^2}_{V_{dc}} + \frac{1}{2} L_{qs} \underbrace{(i_{qs}^{ref} - i_{qs})^2}_{i_{qs}} + F(i_{dqs})$$

$$\lambda_1 = \frac{1}{2} C \overline{V_{dc}}^2 + \frac{1}{2} L_{qs} (\overline{i_{qs}})^2 + F(i_{dqs}) \quad (11)$$

where, the last nonlinear term is expressed as:

$$F(i_{dqs}) = \begin{cases} 0, & i_{dqs} < \text{statorcurrentpeak} \\ \infty, & i_{dqs} > \text{statorcurrentpeak} \end{cases}$$

The strategy ensures stability through a Lyapunov-based cost function. where λ_1 and λ_2 are denoting energy like measures. It is capturing dc-link voltage deviation and stator current tracking performance. Both are composed of quadratic terms, ensuring positive definiteness. This is producing monotonically decreasing at each sampling instant under the optimal switching action. The quadratic terms guarantee convergence of dc-link voltage and current errors. The nonlinear function $F(i_{dqs})$ is producing desired states and prevents limit violations. Hence, the closed-loop system remains stable and trajectories converge without violating current constraints. It is consistent with Lyapunov stability criteria commonly applied in FCS-MPC schemes.

The cost function (λ_1) will be very high, if a particular voltage sector is predicting machine currents with amplitude higher than its peak. As a result, this voltage vector will not be chosen. This criterion is enabling the strategy for not considering all the possible voltage vector for optimal solution. When the dc link voltage converges to the reference voltage (outer PI loop) and reaches a steady state $\frac{dV_{dc}}{dt} = 0$. The cost function is formulated by (11) considering also the voltage regulation effect, which gradually forces the future voltage to accurately track the reference voltage. This control scheme manages the motor current during fault condition with the help of dc link voltage regulation. The addition of the PI dc link controller term eliminates the steady-state error caused by parameter uncertainty.

The predictive control strategy known as one step ahead prediction solves the optimization complexity by searching within the permissible voltage vectors ($n=0$ to 7) to find the optimal one that minimizes the cost function as presented in Fig. 3a. In this case, the total energy declines to zero during the transition of switching states $\{\Delta s = s(k+1) - s(k)\}$. The energy must be dissipated to ensure asymptotic stability. Therefore, by using the Lyapunov energy function during switching state transition is described as:

$$\lambda_2 = \frac{1}{2} \Delta s^2 \frac{V_{dc} E_{sw_loss}}{V_M} \quad (12)$$

where V_M , E_{sw_loss} are the permissible voltage and energy loss given by the manufacture data set.

It is seen that, the switching transitions are non-uniform and event-driven, demonstrating that the controller does not switch at every sampling instant as presented in Fig. 3b, c respectively. Since the controller sampling time is 100 μ s (10 kHz), a switching action at each sample would produce a uniform 10 kHz square wave. However, the measured waveform shows several flat intervals where the switching signal remains in the same state across multiple sampling periods (typically 3–6 consecutive samples). This behavior indicates that the MPC does not update the switching state at every sample, but only when the cost-function selects a different voltage vector as optimal. Consequently, switching events occur less frequently than the sampling events, resulting in an effective switching frequency in the range of 2–5 kHz, which is significantly lower than the 10 kHz sampling rate. This directly confirms that the proposed MPC reduces switching activity and therefore switching losses. As

Denotation	Value
Pole	6
Rated speed (rpm)	1000
Rated power (kW)	1
Stator resistance (Ω)	10.33
Stator inductance (H)	$L_d = 0.0147, L_q = 0.0133$
flux linkage (Wb)	0.5532

Table 1. Specific parameters of the PMSM drive system.

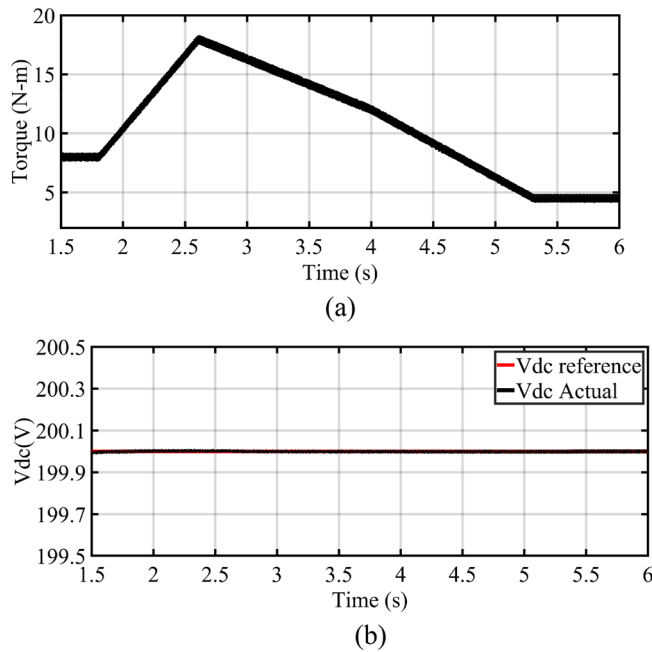


Fig. 4. Performance (a) electromagnetic torque, and (b) dc link voltage due to load perturbation.

illustrated in Fig. 1, the proposed scheme is derived from the d–q model simplified by a model transformation. Based on the adaptive terms, the stability–robustness constraints and predicted state variables are computed with respect to the switching-states from the finite set. Finally, the optimal solution search with respect to the objective function offers an optimal switching-state to be applied into the converter.

Results and discussion

The mathematical analysis of the considered system is realized on MATLAB/Simulink environment. The specific parameters of the prototype are described in Table 1. The overall control algorithm is based on the vector control with step ahead prediction. The sampling time are set as 100 μ s. The parameters of dc- link PI controller is $K_p = 0.5$, $K_i = 0.1$. For a PMSM, the electrical time constant can be derived as per the given motor parameter as:

$$\tau_e = \frac{L_d}{R_s} = \frac{L_q}{R_s} \approx 1.2 \text{ ms}$$

As per control criterion, controller will be sample at least 10–15 times faster than the electrical time constant:

$$T_s \leq \frac{\tau_e}{10} \approx 120 \mu\text{s}$$

$$T_s = 100 \mu\text{s} \leq \frac{\tau_e}{10}$$

This ensures sufficiently fine discretization of the model for MPC prediction accuracy.

The data depicted in Fig. 4 reveals that the dynamic response times for PMSM involving abrupt changes in torque loads. As it can be seen from Fig. 4a, the electromagnetic torque settling time during the load variation is almost negligible. The dynamic response of the torque is giving clear convenient idea regarding the robustness feature of controller. It is noteworthy that the d-axis component of the stator stays at zero value i.e. remain invariant during accelerating and decelerating and constant speed mode. In contrast, the q-axis current

exhibits to the changes, especially at the abrupt shift of load torque as depicted in Fig. 5a. During this scenario the dc link voltage is following the set value at 200 V. There is negligible deviation as shown in Fig. 4b during perturbation keeping the source end invariant.

The data depicted in Fig. 5 reveals that the active power component of the machine i.e. q-axis component have faster response time and better dynamic-state performance. Hence, the dynamic performance can be improved under heavy load disturbance with the designed control scheme.

Additionally, the current ripple in d-axis is 1 mA, with no static error in q-axis current as shown in Fig. 5b.

In conclusion, the results for load disturbance affirm that the proposed methodology has better dynamic state controllability as the convention scheme can avoid the current error and obtain faster response time for speed variation to achieve better dynamic-state performance.

The predictive control scheme requires the system parameters. It is seen that stator inductance and resistance have an effect on the designed method, respectively. In order to check the efficacy and parametric sensitivity of the proposed technique, the optimized objective function is considered for variations.

The system has been investigated under the both inductance variations of 1.5 time to 10 times of its measured actual values as shown in Fig. 6a. It is observed that the machine current is following the set value with negligible ripple content as shown in Fig. 6b, c respectively. The q-axis current at 2 s is presented in Fig. 6b. The multi objective function is able to remove the uncertainty caused by the zoomed view of the q-axis current during variation of dq-axis parameter successfully as reflected here. The THDs of the machine currents are equal to 3.82% as shown in Fig. 6e. During this wide variation, the dc link controller is able to maintain the power flow between source and load end with negligible disturbance as presented in Fig. 6d.

Similarly, another scenario, due to ageing of stator resistance, the effect the machine variables are shown in Fig. 7a. It is seen that the errors are minimal and also cause no alteration in the torque profile as depicted in Fig. 7b. This means that the proposed controller is devoid of the existence in any motor parameters. This adaptive method significantly augments the precision and robustness of the nonlinear constraints in the strategy, including peak current limits as shown in Fig. 7b, c respectively. The dc-link voltage remain unaltered at 200 V with negligible deviation as presented in Fig. 7d.

This scenario represents practical operating conditions of PMSMs, where temperature rise increases R_s while magnetic saturation alters both L_d and L_q at the same time. The variations of the machine parameters considered in this study range from 50 to 150% of their nominal values, as depicted in Fig. 8a. As it can be observed, even under abrupt and large simultaneous deviations of the parametric values from the nominal, the dc-link voltage remains maintained at 200 V with negligible deviation as presented in Fig. 8b. The q-axis stator current is following its reference accurately, with only a slight increase in ripple due to the mismatch as portrayed in Fig. 8c. Statistically, the standard deviation of the q-axis stator current component remains well within 1.0283%. Similarly, the d-axis current remains close to zero (note: as the rotor is made of permanent magnet) without any steady-state deviation as presented in Fig. 8d. These results confirm that the proposed predictive control strategy.

During variation of both stator resistance and inductance behavior of d,q axis current error are shown in Fig. 9a, b respectively. It is observed that the objective function is able to minimize the ripple content in the current successfully by keeping the current within permissible limit. In conclusion, the vital benefit of the

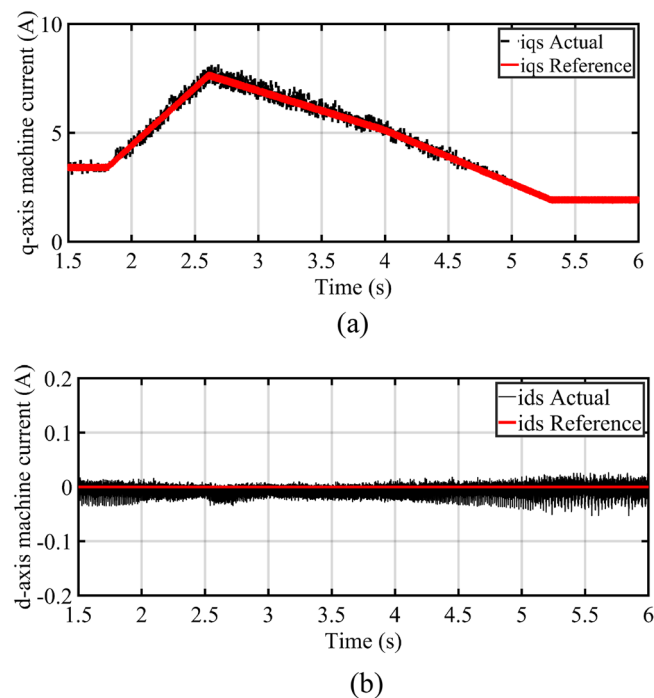


Fig. 5. Behavior of (a) q-axis (b) d-axis machine current due to load perturbation.

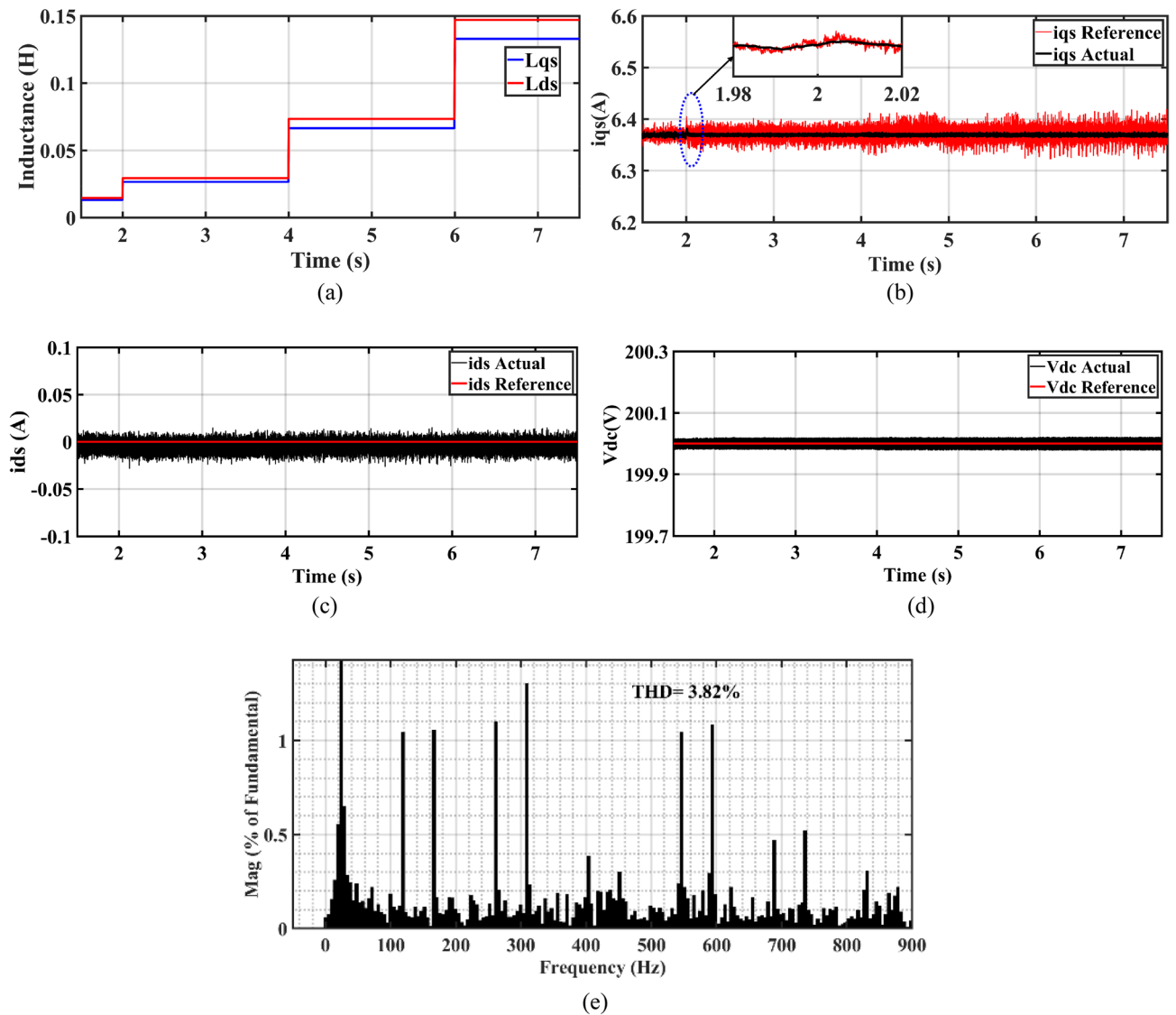


Fig. 6. During variation of inductance (a) Variation of q,d-axis inductance (b)Q-axis machine current (c) d-axis component of machine current (d) dc link voltage (e) FFT analysis of stator current.

scheme resides in its ability to effectively reimburse for nonlinearities in the machine under abrupt variation of different circumstances. By integrating laboratory tested stator inductance, the system permits more precise regulations, minimizing the static errors between the sampled and step ahead variables. This predictive scheme uninterruptedly updates the variations in the dynamic state of the model.

Another scenario with simultaneous changing the flux, stator resistance and inductance at double the rated value at constant.

load torque has been applied to the PMSM drive. As it can be seen that the dc-link voltage experiences a negligible disturbance as presented in Fig. 10a. The torque and flux component of the machine current tends to follow the set value with fast transient time as presented in Fig. 10b, c respectively. Also, negligible ripple component is existing during these deviations.

The computational burden of the scheme is assessed based on the computation time of the code during simulation study. The multi- objective cost minimization involves dc link voltage error, switching loss minimization term, and stator current error to generate the optimal voltage vector. This scheme doesn't include all the 6 possible active voltage vectors for gating the switching signal of 2 level converter. So the computational burden is little less as shown in Fig. 11. However, the sampling period of the considered work is 100 microseconds, so the computation time of the proposed method will not affect the performance of the system.

Conclusion

This paper presents the development of a predictive control strategy for PMSM systems. By employing a multi objective cost function within the MPC framework, the model seamlessly handles nonlinear constraints, ensuring precise control over both load perturbation and motor parameter uncertainty. Through the formulated strategy

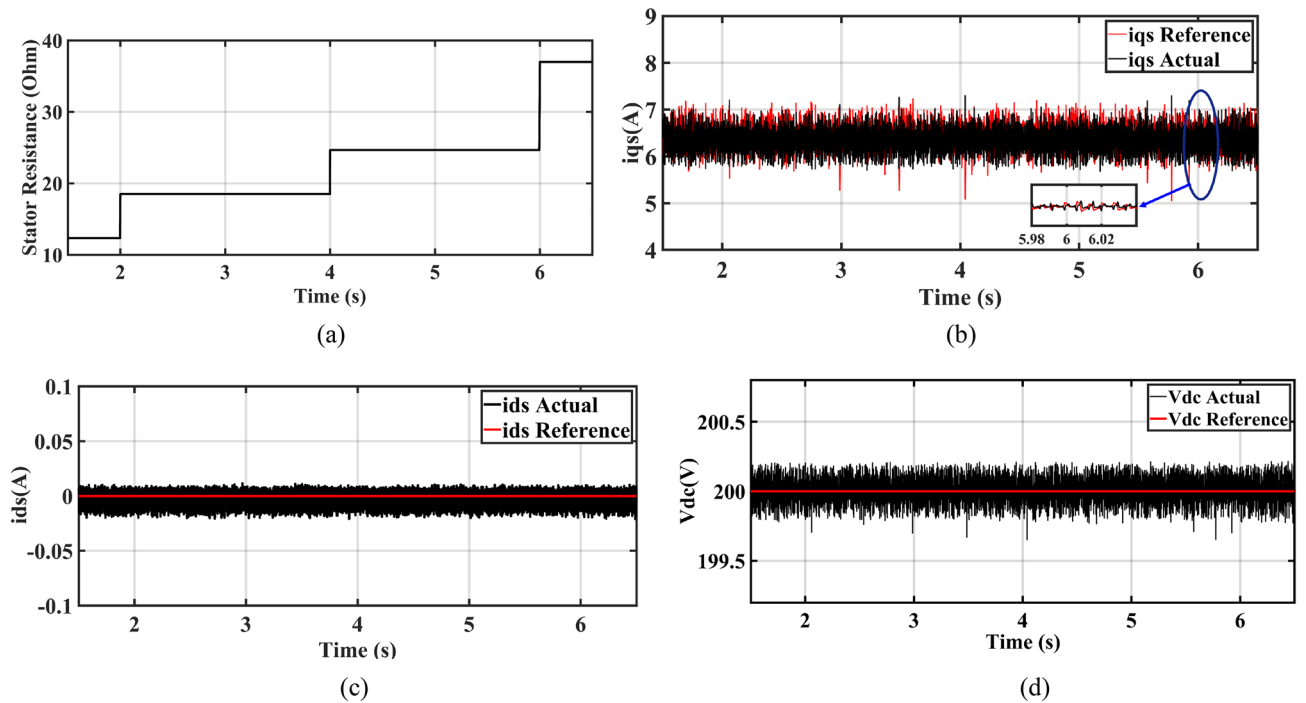


Fig. 7. During variation of resistance (a) Variation of stator resistance (b) Q-axis machine current (c) d-axis component of machine current (d) dc link voltage.

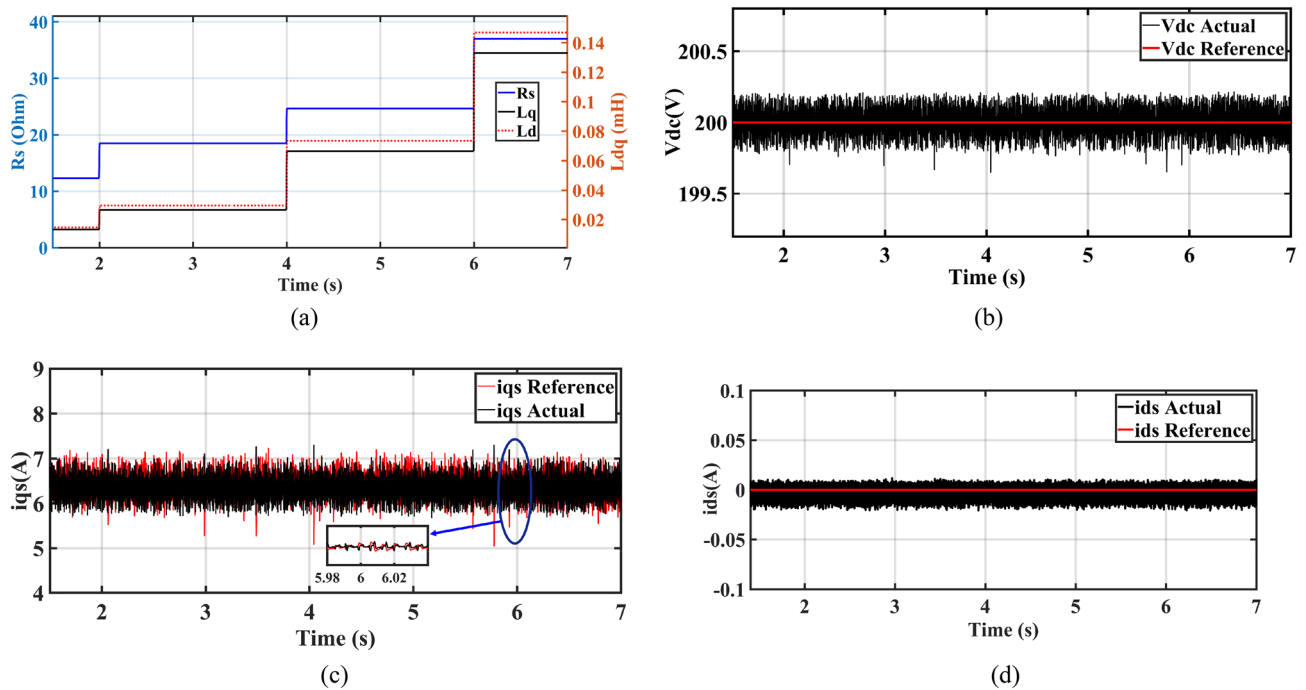


Fig. 8. During simultaneous variation in stator resistance and inductance effect of (a) variation of R_s , L_{dq} (b) dc link voltage (c) q-axis stator current (d) d-axis stator current.

rhythm, the objective function factor is calculated using the predictive errors of dq-axis current and applied to generate the optimal voltage vector. The scheme dynamically eliminates some of the candidate voltage vector before they are evaluated by MPC with the application of nonlinear term in the cost function. So computational burden is reduced for the considered system. The mathematical claims with the simulation counterparts show that the method guarantees stability and has better dynamic performance in operating scenarios. The current

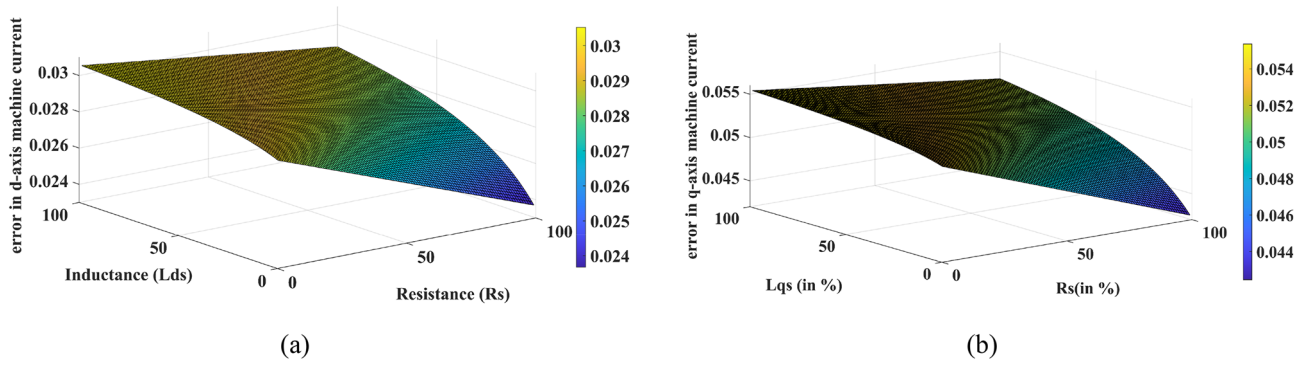


Fig. 9. During % variation of stator resistance and inductance behavior of (a) d-axis error current (b) q-axis error current.

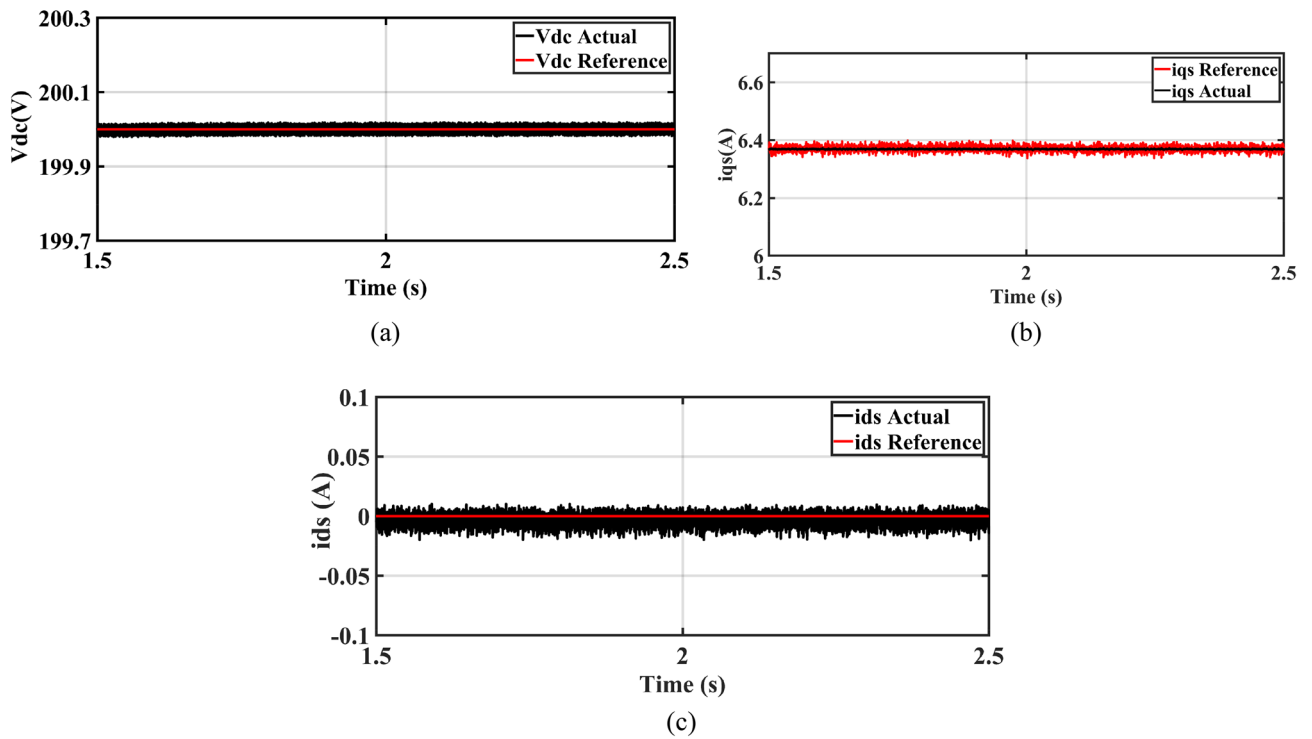


Fig. 10. During $\phi_f = 2\phi_f, R_s = 2R_s, L_s = 2L_s$ Behavior of (a) dc link voltage (b) q-axis machine current (c) d-axis machine current.

THD is able to maintain within 5% even during parameter mismatching condition. This work can be extended in real-world challenging across different EVs to confirm the robustness of the strategy, and applying multi-objective cost function to further enhance efficiency and battery life.

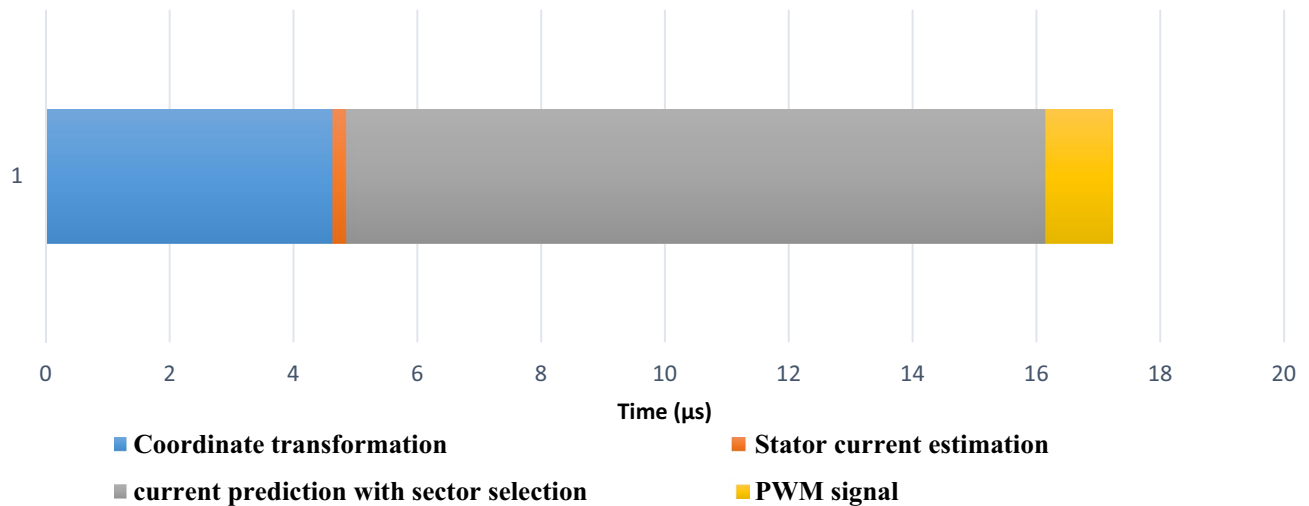


Fig. 11. Computational estimation of the considered scheme.

Data availability

All data generated or analyzed during this study are included in this article.

Received: 23 August 2025; Accepted: 31 January 2026

Published online: 27 February 2026

References

- Salem, A. & Narimani, M. A review on multiphase drives for automotive traction applications. *IEEE Transact. Transport. Electr.* **5**(4), 1329–1348 (2019).
- Yang, Z., Shang, F., Brown, I. P. & Krishnamurthy, M. Comparative study of interior permanent magnet, induction, and switched reluctance motor drives for EV and HEV applications. *IEEE Trans. Transp. Electr.* **1**(3), 245–254 (2015).
- Im, J.-H. & Kim, R.-Y. 'Improved saliency-based position sensorless control of interior permanent-magnet synchronous machines with single dc-link current sensor using current prediction method'. *IEEE Trans. Ind. Electron.* **65**(7), 5335–5343 (2018).
- Chen, P. & Luo, Y. Analytical fractional-order PID controller design with bode's ideal cutoff filter for PMSM speed servo system. *IEEE Trans. Ind. Electron.* **70**(2), 1783–1793 (2023).
- Yin, Z., Gong, L., Du, C., Liu, J. & Zhong, Y. Integrated position and speed loops under sliding-mode control optimized by differential evolution algorithm for PMSM drives. *IEEE Trans. Power Electron.* **34**(9), 8994–9005 (2019).
- Wang, F. & He, L. FPGA-based predictive speed control for PMSM system using integral sliding-mode disturbance observer. *IEEE Trans. Ind. Electron.* **68**(2), 972–981 (2021).
- Niu, F., Li, K. & Wang, Y. Direct torque control for permanent magnet synchronous machines based on duty ratio modulation. *IEEE Trans. Ind. Electron.* **62**(10), 6160–6170 (2015).
- Vazquez, S. et al. Model predictive control for power converters and drives: advances and trends. *IEEE Trans. Ind. Electron.* **64**(2), 935–947 (2017).
- Wang, F. et al. High performance model predictive control for pmsm system using Bayesian ascent and Gaussian process. *IEEE Trans. Energy Convers.* **39**(2), 851–861 (2024).
- Ismail, M. M., Xu, W., GeJ, T. Y., Junejo, A. K. & Hussien, M. G. Adaptive linear predictive model of an improved predictive control of permanent magnet synchronous motor over different speed regions. *IEEE Trans. Power Electron.* **37**, 15338–15355 (2022).
- Zhao, M., Zhang, S., Zhang, C., Li, X. & Dong, Y. A parameter robust finite control set model predictive current control based on incremental prediction model for SPMSM drives. *IEEE J. Emerg. Select. Topics Ind. Electron.* **5**(3), 1292–1302 (2024).
- Sun, Z. et al. Finite control set model-free predictive current control of PMSM with two voltage vectors based on ultralocal model. *IEEE Trans. Power Electron.* **38**(1), 776–788 (2023).
- Wu, X. et al. Equivalent three-vector-based model predictive control with duty-cycle reconstruction for PMSM. *IEEE Trans. Ind. Electron.* **71**(3), 2395–2404 (2024).
- Yan, L. et al. Suppression of major current harmonics for dual three-phase PMSMs by virtual multi three-phase systems. *IEEE Trans. Industr. Electron.* **69**(6), 5478–5490 (2022).
- Chen, Z. & Qiu, J. Adjacent-vector-based model predictive control for permanent magnet synchronous motors with full model estimation. *IEEE J. Emerg. Sel. Topics Power Electron.* **11**(2), 1317–1331 (2023).
- Yang, Y. et al. An efficient model predictive control using virtual voltage vectors for three-phase three-level converters with constant switching frequency. *IEEE Trans. Ind. Electron.* **69**(4), 3998–4009 (2022).

Author contributions

Biplab Kumar Mohapatra: Design and Conceptualization Vidit Sharma: Modelling and analysis Pritam Bhowmik: Drafting, Analysis Rupa Mishra: Supervision, Conceptualization.

Funding

Open access funding provided by Vellore Institute of Technology.

Declarations

Competing interests

The authors declare no competing interests.

Additional information

Correspondence and requests for materials should be addressed to R.M.

Reprints and permissions information is available at www.nature.com/reprints.

Publisher's note Springer Nature remains neutral with regard to jurisdictional claims in published maps and institutional affiliations.

Open Access This article is licensed under a Creative Commons Attribution-NonCommercial-NoDerivatives 4.0 International License, which permits any non-commercial use, sharing, distribution and reproduction in any medium or format, as long as you give appropriate credit to the original author(s) and the source, provide a link to the Creative Commons licence, and indicate if you modified the licensed material. You do not have permission under this licence to share adapted material derived from this article or parts of it. The images or other third party material in this article are included in the article's Creative Commons licence, unless indicated otherwise in a credit line to the material. If material is not included in the article's Creative Commons licence and your intended use is not permitted by statutory regulation or exceeds the permitted use, you will need to obtain permission directly from the copyright holder. To view a copy of this licence, visit <http://creativecommons.org/licenses/by-nc-nd/4.0/>.

© The Author(s) 2026